Video Article

Atomic Scale Structural Studies of Macromolecular Assemblies by Solid-state Nuclear Magnetic Resonance Spectroscopy

Antoine Loquet[1], James Tolchard[1], Melanie Berbon[1], Denis Martinez[1], Birgit Habenstein[1]

[1]Institute of Chemistry, Biology of Membranes, Nanoobjects, UMR5248 CNRS, Université de Bordeaux

Correspondence to: Antoine Loquet at antoine.loquet@u-bordeaux.fr, Birgit Habenstein at birgit.habenstein@u-bordeaux.fr

URL: https://www.jove.com/video/55779
DOI: doi:10.3791/55779

Keywords: Biochemistry, Issue 127, Structural biology, macromolecular assemblies, nuclear magnetic resonance, solid-state NMR, magic-angle spinning, self-assemblies, protein complexes, amyloid fibrils, bacterial filaments

Date Published: 9/17/2017

Citation: Loquet, A., Tolchard, J., Berbon, M., Martinez, D., Habenstein, B. Atomic Scale Structural Studies of Macromolecular Assemblies by Solid-state Nuclear Magnetic Resonance Spectroscopy. *J. Vis. Exp.* (127), e55779, doi:10.3791/55779 (2017).

Abstract

Supramolecular protein assemblies play fundamental roles in biological processes ranging from host-pathogen interaction, viral infection to the propagation of neurodegenerative disorders. Such assemblies consist in multiple protein subunits organized in a non-covalent way to form large macromolecular objects that can execute a variety of cellular functions or cause detrimental consequences. Atomic insights into the assembly mechanisms and the functioning of those macromolecular assemblies remain often scarce since their inherent insolubility and non-crystallinity often drastically reduces the quality of the data obtained from most techniques used in structural biology, such as X-ray crystallography and solution Nuclear Magnetic Resonance (NMR). We here present magic-angle spinning solid-state NMR spectroscopy (SSNMR) as a powerful method to investigate structures of macromolecular assemblies at atomic resolution. SSNMR can reveal atomic details on the assembled complex without size and solubility limitations. The protocol presented here describes the essential steps from the production of $^{13}C/^{15}N$ isotope-labeled macromolecular protein assemblies to the acquisition of standard SSNMR spectra and their analysis and interpretation. As an example, we show the pipeline of a SSNMR structural analysis of a filamentous protein assembly.

Video Link

The video component of this article can be found at https://www.jove.com/video/55779/

Introduction

Advances in magic-angle spinning solid-state nuclear magnetic resonance spectroscopy (SSNMR) offer an efficient tool for the structural characterization of macromolecular protein assemblies at an atomic resolution. These protein assemblies are ubiquitous systems that play essential roles in many biological processes. Their molecular structures, interactions and dynamics are accessible by SSNMR studies, as has been shown for viral (capsids[1]) and bacterial infection mechanisms (secretion systems[2,3], pili[4]), membrane protein complexes[5,6,7,8] and functional amyloids [9,10,11]. This type of molecular assembly can also provoke pathologies such as in neurodegenerative diseases where proteins assemble in misfolded, amyloid states and cause aberrant cell behavior or cell death [12,13]. Protein assemblies are often built by the symmetric oligomerization of multiples copies of protein subunits into large supramolecular objects of various shapes including fibrils, filaments, pores, tubes, or nanoparticles. The quaternary architecture is defined by weak interactions between protein subunits to organize the spatial and temporal assembly and to allow for sophisticated biological functions. Structural investigations at an atomic scale on these assemblies are a challenge for high-resolution techniques since their intrinsic insolubility and very often their non-crystallinity restricts the use of conventional X-ray crystallography or solution NMR approaches. Magic-angle spinning (MAS) SSNMR is an emerging technique to obtain atomic resolution data on insoluble macromolecular assemblies and has proven its efficiency to resolve 3D atomic models for an increasing number of complex biomolecular systems including bacterial filaments, amyloid assemblies and viral particles [14,15,16,17,18,19,20,21,22]. Technical advances on high magnetic fields, methodological developments and sample preparation has established MAS SSNMR into a robust method to investigate insoluble proteins in various environments, notably in their biologically-relevant macromolecular assembled state or in cellular membranes, making the technique highly complementary to cryo-electron microscopy. In many cases, a very high degree of symmetry characterizes such protein assemblies. MAS SSNMR exploits this feature, as all protein subunits in a homomolecular assembly would have the same local structure and therefore virtually the same SSNMR signature, drastically reducing the complexity of the analysis.

An efficient protocol for structural studies of macromolecular protein assemblies by moderate MAS (<25 kHz) SSNMR is presented in this video and can be subdivided into different steps (**Figure 1**). We will demonstrate the critical stages of the workflow of a SSNMR structural study exemplified on a filamentous protein assembly (see highlighted steps in **Figure 1**), with the exception of protein subunit purification, differing for each protein assembly but of critical importance for structural studies, and without going into the technical/methodological details of SSNMR spectroscopy and structure calculation for what specialized tutorials are available online. While the present protocol will primarily focus on solid-state NMR experiments performed under MAS conditions, the use of aligned biological environments [23,24,25,26,27], such as aligned bicelles, allow for the investigation of protein conformation and dynamic protein-protein interaction in membrane-like media without MAS technology. We will show the protein expression and assembly steps as well as the recording of the crucial SSNMR spectra and their analysis and interpretation.

Our aim is to provide insights into the structural analysis pipeline enabling the reader to perform an atomic-resolution structural study of a macromolecular assembly by SSNMR techniques.

The protocol encompasses 3 sections:

1. Solid-state NMR sample production

As a prerequisite to a solid-state NMR analysis, the protein components of the macromolecular assembly need to be expressed, isotope-labeled, purified and assembled *in vitro* into the native-like complex state (for an example see **Figure 2**). To ensure high NMR sensitivity, isotope enrichment in ^{13}C and ^{15}N labeling is required through the use of minimal bacterial expression media supplemented with ^{13}C and ^{15}N sources, such as uniformly ^{13}C-labeled glucose/glycerol and $^{15}NH_4Cl$ respectively. In the later stage of the protocol, selectively ^{13}C-labeled samples produced with selectively ^{13}C-labeled sources such as (1,3-^{13}C)- and (2-^{13}C)-glycerol (or (1-^{13}C)- and (2-^{13}C)-glucose) are used to facilitate the NMR analysis. Mixed labeled sample corresponding to an equimolar mixture of either 50% ^{15}N- and 50% ^{13}C-labeled or 50% (1,3-^{13}C)- and 50% (2-^{13}C)-glucose are introduced to describe the detection of intermolecular interactions. A high degree of protein purity as well as rigorous conditions during the assembly step are key factors to insure a homogeneous structural order of the final sample.

2. Preliminary structural characterization based on one-dimensional (1D) solid-state NMR

We present the essential experiments for a structural analysis by SSNMR. One-dimensional (1D) cross-polarization (CP) and INEPT / RINEPT[28] experiments, detected on ^{13}C nuclei are used to detect rigid and flexible protein segments in the assembly, respectively, and to estimate the degree of structural homogeneity and local polymorphism (for an example see **Figure 3**).

3. Conformational analysis and 3D structure determination

Subsections 1 and 2 concern the conformational analysis, which is based on the SSNMR resonance assignment of all rigid residues of the protein assembly, as the chemical shifts are very sensitive probes to the local environment and can be used to predict the phi/psi dihedral angles and thereby determine the secondary structure. **Figure 4** illustrates an example of a sequential resonance assignment in the rigid core of a protein assembly**.** The 3D structure determination is based on the collection of structural data such as distance restraints encoding close proximities (<7 - 9 Å), containing both intra- and intermolecular information. Subsections 3 and 4 describe long-range distant restraint collection and interpretation. Long-range contacts are defined as intramolecular ^{13}C-^{13}C proximities arising from residue i to j, with |i-j| ≥4, defining thereby the tertiary protein fold of the monomeric subunit, or as intermolecular ^{13}C-^{13}C proximities, defining the intermolecular interfaces between protein subunits in the assembly. Intra- and intermolecular interfaces are illustrated in **Figure 5**. SSNMR restraints detected through ^{13}C-^{13}C and ^{15}N-^{13}C recoupling experiments usually encode for internuclear distances < 1 nm. Subsection 4 explains the detection of intermolecular distance restraints. In symmetrical protein assemblies, the use of homogeneously labeled samples (*i.e.* 100% uniformly or selectively labeled) for identifying intermolecular subunit-subunit interactions is limited, as both intra- and inter-molecular contacts lead to detectable signals. The unambiguous detection of intermolecular proximities is achieved by using mixed labeled samples, containing an equimolar mixture of two differently labeled samples, combined prior to aggregation. Subsection 5 briefly introduces structure modeling.

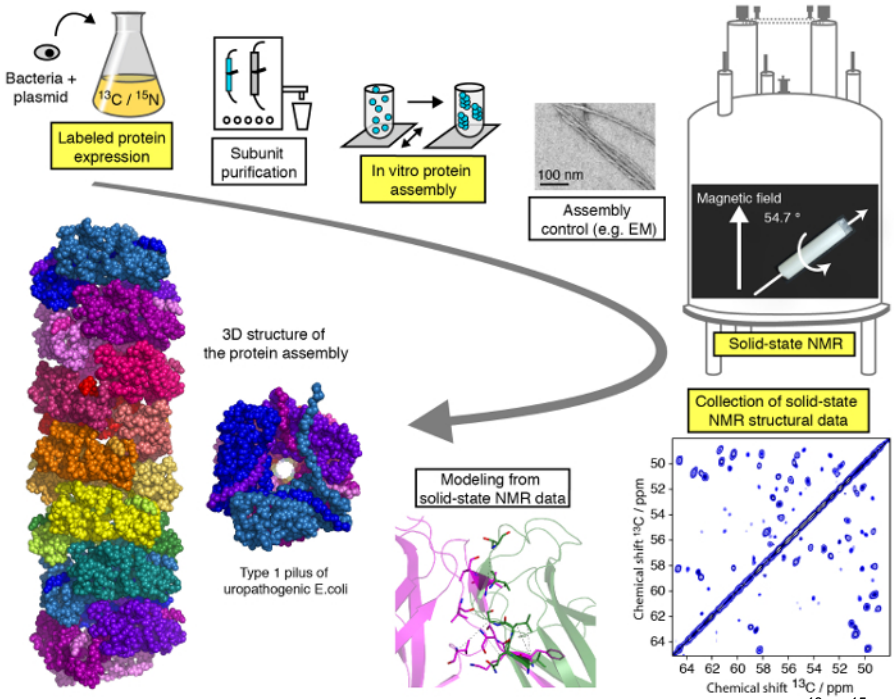

Figure 1: Workflow of an atomic-resolution structural study by solid-state NMR. ^{13}C, ^{15}N isotope labeled protein production, subunit purification, subunit assembly, control of assembly formation, SSNMR experiments, SSNMR experiment analysis and extraction of distance restraints, and structure modeling are shown. Please click here to view a larger version of this figure.

Protocol

1. Solid-state NMR sample productiona

1. **Production of uniformly $^{13}C/^{15}N$-labeled protein subunits**
   1. Use freshly transformed, pET24-peptide-6his plasmid-containing *E. coli* BL21 (DE3) cells, harvest them from the prepared agar plate.
   2. Inoculate a 15 mL pre-culture of pre-warmed LB medium with one colony. Incubate at 37 °C with 200 rpm shaking overnight.
   3. Transfer the pre-culture into 1 L of the main culture of pre-warmed M9 medium (see composition in **Table 1**), containing the required isotope-labeled carbon and nitrogen sources.
      NOTE: This can be uniformly ^{13}C-labeled glucose, selectively (1-^{13}C)- or (2-^{13}C)-labeled glucose [29,30,31] or (1,3-^{13}C)- or (2-^{13}C)-labeled glycerol[32,33].
   4. Incubate this at 37 °C and measure the OD_{600} as soon as the culture becomes turbid. When the OD_{600} has reached a value of 0.8, induce protein expression with 0.75 mM IPTG for 4 h.
      NOTE: The optimal induction conditions can vary from one protein to another.
   5. Recover the cells by centrifugation for 30 min at 6000 x g and 4 °C.

2. **Purification sketch** (not shown in the video protocol)
   1. Lyse cells using standard techniques such as sonication or lysozyme treatment and purify the protein subunit using techniques established or adapted for the investigated protein assembly.
      NOTE: The protein can be expressed in inclusion bodies, check for the protein localization by cell lysis and subsequent centrifugation. If the protein is found in the sediment with the cell debris, it has been accumulated in inclusion bodies.
   2. Test expression and purity of the protein sample for example by a standard 12-15% Tris-Tricine SDS-PAGE, see **Figure 2A**. If the purity is sufficient, the protein can be assembled, otherwise perform a supplementary purification step.

3. ***In vitro* assembly of the protein filaments**
   1. Check protein concentration in the purified solution. If the protein contains absorbing residues, measure the absorption in a UV spectrophotometer at 280 nm. Insert the pure buffer into the spectrophotometer as calibration and measure then the protein absorbance.
   2. Calculate the protein concentration using the absorption coefficient of the protein subunit with the adapted Beer-Lambert law: $A_\lambda=\varepsilon_\lambda$ x l x c; here A is the optical density at a given wave-length λ; ε is the specific absorption coefficient; l is the length of the optical trajectory in cm; c is the concentration in mol/L.
   3. Concentrate the protein to a concentration of 1 mM in a centrifugal filter unit. Introduce the sample into the centrifugal filter unit and centrifuge at 4000 x g for 30 min, mix the solution in the filter unit gently with a pipet to avoid protein deposition at the filter. Repeat the procedure until the desired concentration is reached.
      NOTE: The optimal assembly concentration depends on the system and needs to be optimized (usually between 0.1 - 1 mM). If an equimolar mixed labeled sample of two different labeled protein batches is prepared (*e.g.* (50/50) (U-^{15}N)-/(U-^{13}C)-labeled), mixing must take place either before or right after the concentration step to ensure homogenization of the mixed solution.
   4. Transfer the sample into a tube and incubate it under agitation for one week at room temperature.
   5. Usually the polymerization of the subunits into filaments is accompanied by the solution becoming turbid. Check the microscopic fibril morphology and homogeneity for example by electron microscopy (magnification 6300X - 45000X), see **Figure 2B**.
   6. Centrifuge the sample for 1 h at 20000 x g and 4 °C. Remove the majority of the supernatant, leave only enough liquid to cover the surface to avoid sample drying. Check the supernatant for non-assembled subunits on the UV spectrophotometer.
   7. Wash the sample by adding H_2O and careful resuspend the content with a pipette. Do not vortex. Spin the sample for 30 min at 22000 x g and 4 °C. Repeat the washing step 3 times. Check during all washing steps if the pellet preserves its aspect after centrifugation and check the supernatant for non-assembled subunits on the UV spectrophotometer.
   8. Add 0.02% (w/v) sodium azide (NaN_3) to avoid bacterial contamination and store the sample until measurement at 4 °C.

4. **Solid-state NMR rotor filling**
   1. Centrifuge twice for 30 min at 22000 x g and 4 °C. Remove maximum amount of the supernatant; the resulting sample consistency depends on the protein assembly, and is usually a gel-like deposit.
   2. Use a capillary pipet to insert the sample into the SSNMR rotor.
      NOTE: Here, we present the procedure on a 4 mm diameter rotor.
      1. Centrifuge the rotor on a table centrifuge to gently introduce the sample into the rotor. Repeat the procedure until the rotor is filled up. Keep minimum space to close the rotor with the rotor cap. If the sample quantity is not sufficient, introduce a commercially available insert to fill up the remaining space to ensure the sample distribution homogeneity in the rotor.
         NOTE: Dependent on the assembled sample consistency, it might be more adequate to use a thin spatula, especially for very dense samples. Rotors with diameters of 2.5 to 4 mm are used at moderate MAS frequencies.
   3. Add traces of 4,4-dimethyl-4-silapentane-1-sulfonic acid (DSS) for internal chemical shift and temperature calibration.
   4. Close the cap with a closing device.
   5. Check under a magnifier if the cap is well inserted and completely closed.

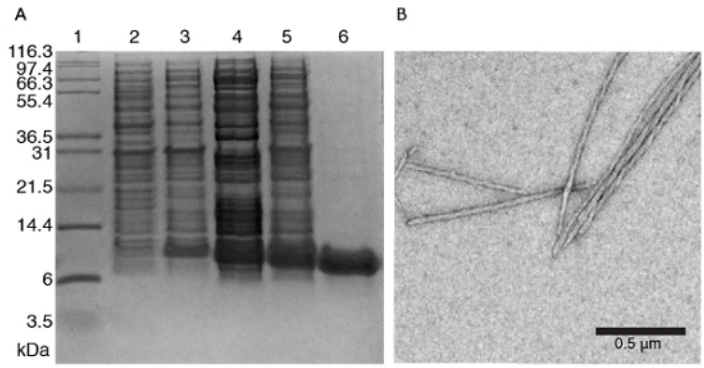

Figure 2: Representative results for protein subunit purification and assembly. A) 15% Tris-tricine SDS-PAGE of protein subunit (including His_6-tag) at different stages of purification. Lane 1 - Protein molecular weight marker; lane 2 - *E. coli* BL21 (DE3) cells uninduced control; lane 3 - *E. coli* BL21 (DE3) cells induced with 0.75 mM IPTG; lane 4 - solubilized inclusion bodies lane 5 - supernatant fractions of cell lysate; lane 6 - purified fraction after Nickel immobilized metal affinity chromatography (IMAC) FPLC and desalting. B) Negatively stained protein fibrils by TEM imaging. Please click here to view a larger version of this figure.

2. Preliminary structural characterization based on one-dimensional (1D) solid-state NMR

1. **Initial set-up and 1D cross-polarization (CP)**
    1. Insert the rotor into the NMR magnet
    2. Start to spin the rotor at a frequency of 5 kHz and wait for a stabilization of ±10 Hz, then accelerate until 7 kHz. Tune and match ^{1}H, ^{13}C and ^{15}N channels. Set the temperature to 2-10 °C (275-283 K); sample heating at 7 kHz MAS is low and temperature adjustment is usually not required at this MAS frequency.
    3. Record a single-pulsed 1D ^{1}H spectrum using 16 scans.
    NOTE: Power levels must have previously been optimized on a reference compound (such as a $^{13}C/^{15}N$ histidine or glycine),to provide starting values for optimizing the power levels in the experiments on the target sample; this procedure is a routine task and therefore out of scope in this protocol.
    4. Keep the temperature during all experiments between 2-10 °C, in hydrated samples the temperature is reflected in the relative shift of the bulk water ^{1}H resonance with respect to the DSS signal[34]. Measure the temperature following the relationship $\delta(H_2O) = 7.83-T/96.9$ with a precision of 1 - 2 °C[35].
    5. Set up the desired MAS frequency and wait until stabilization of ±10 Hz.
    NOTE: Here it is demonstrated for a frequency of 11 kHz.
    6. Tune and match ^{1}H and ^{13}C channels again and adjust the temperature with the help of a 1D ^{1}H experiment.
    7. Set up a 1D ^{1}H-^{13}C CP[36].
    NOTE: CP experiments show the signals arising from residues in a rigid conformation. Pulse calibration and decoupling parameters can be directly optimized on the sample when the sensitivity is high enough to observe signals after less than ~32 scans. The initial optimization values are taken over from the standard optimization on a reference compound. CP contact time and power levels are chosen based on maximal signal intensity. In protein samples, the optimal CP contact time is usually between 200 µs and 2 ms. The decoupling parameters should also be re-adjusted from the calibration on a reference compound.
        1. Carefully observe the localization of spinning sidebands at the given MAS frequency.
    8. Record a reference 1D ^{13}C CP spectrum that serves as 1D spectral fingerprint. Typical parameters are 128 scans, 1 ms CP contact time, 100 kHz decoupling strength, a recycle delay of 3 s and 25 ms of acquisition.
    9. Calibrate the ^{1}H and ^{13}C chemical shifts following the IUPAC recommendations[37]. Determine the resonance frequency of the ^{1}H DSS signal (chemical shift of 0 ppm); ^{13}C chemical shifts are referenced to ^{1}H shifts (usually ~0.25144, derived from the ratio of the ^{13}C to the ^{1}H resonance frequency[37]).
    10. Process the 1D ^{1}H-^{13}C CP experiment without apodization function (see **Figure 3A** and **B** for the detection on a homogeneously well-ordered protein assembly). Choose an isolated peak to estimate the linewidth in the sample, indicative of structural order and homogeneity. Typical ^{13}C linewidths for well-ordered biological protein assemblies under MAS at high magnetic fields range between 20 - 150 Hz (measured as the full-width at half-height (FWHH)).
    11. Estimate the signal-to-noise (S/N) ratio in the CP spectrum.
    NOTE: The S/N ratio depends on many factors, including mainly the amount of sample in the rotor, the degree of rigidity of the protein structure and the presence of a single molecular conformation. As a rule of thumb, a sample should be suitable for multidimensional SSNMR spectroscopy if a signal is observed in an optimized 1D ^{1}H-^{13}C CP spectrum recorded with 64 scans.
    12. Zoom into the spectral region of the protein backbone carbonyl resonances (mainly) localized between 165 - 180 ppm. Estimate the secondary structure content in the assembly by the position of the protein backbone carbonyl resonances with resonances from residues in α-helical or β-strand conformation shifted downfield or upfield, respectively (see **Figure 3B** for a mostly α-helical subunit)[38].

2. **1D INEPT experiment**
    1. Set up a 1D ^{1}H-^{13}C INEPT experiment to probe highly mobile parts (sub-µs) of the protein assembly.
    NOTE: GARP decoupling of a few kHz during acquisition[39] is commonly used, to allow for short interscan delays (typically 1 s) without damaging the probe.
    2. Record a reference INEPT spectrum that serves as fingerprint for the mobile protein segments; typical parameters are 128 scans and an acquisition time of 25 ms.

3. Process the ^{1}H-^{13}C INEPT experiment. The amount and the positions of the signals are indicative of the amount of mobile residues and the amino acid composition respectively.
   NOTE: Also record a 2D ^{1}H-^{13}C INEPT experiment if signals are present in the 1D INEPT spectrum (see **Figure 3C** for an example) to permit a more specific amino acid identification. In ambiguous assignment cases, we recommend checking the buffer component signal positions by solution NMR.
4. Use the BMRB database[40] and published data[38] to assign the resonances to their corresponding amino acid in near random coil conformation; the spectrum contains only mobile buffer components if no residues are in a highly mobile regime.

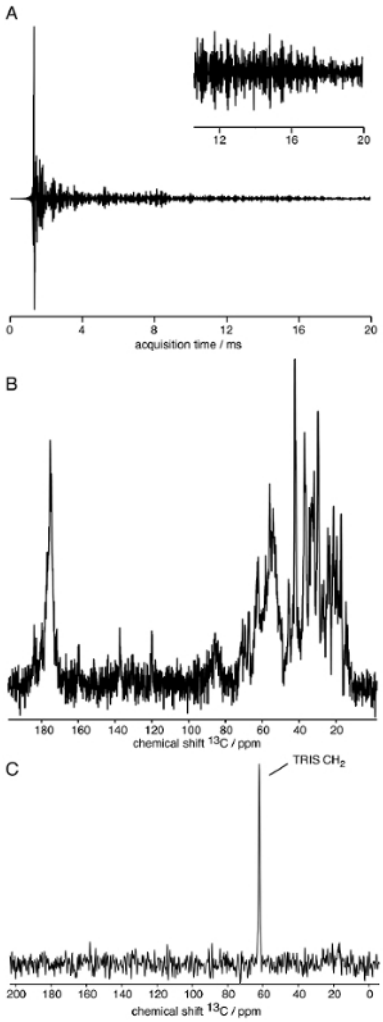

Figure 3: Representative results of SSNMR spectra acquisition for a well-structured protein assembly. A) ^{13}C-detected FID of a ^{1}H-^{13}C cross-polarization experiment. B) ^{1}H-^{13}C cross-polarization experiment. C) ^{1}H-^{13}C INEPT experiment of a rigid protein assembly; only buffer components are visible. Please click here to view a larger version of this figure.

3. Conformational analysis and 3D structure determination

1. **Sequential resonance assignment**
   1. Set up a 2D ^{13}C-^{13}C proton-driven spin diffusion (PDSD)[41] experiment to detect intra-residue ^{13}C-^{13}C correlations, including side chains. Take over the values for the initial ^{1}H-^{13}C cross-polarization step from the 1D ^{1}H-^{13}C CP experiment.
      1. Set the mixing time to 50 ms for uniformly ^{13}C-labeled samples and to 100 ms for selectively ^{13}C-labeled samples. Set the indirect acquisition time between 5 - 25 ms and the direct acquisition between 15-25 ms dependent on the intrinsic spectral resolution, which can be estimated by the visible signal in the Free Induction Decay (FID) length (exemplified in **Figure 3A**).
      2. Test several processing parameters to find optimal values with respect to signal-to-noise and resolution in the spectrum, typically adequate processing can be achieved using a qsine window function with a sine bell shift (SSB) of 2.5-4.
   2. Set up, record and process a 2D ^{13}C-^{13}C PDSD with an intermediate mixing time experiment to detect sequential ^{13}C-^{13}C correlations connecting mostly i - i±1, but also i±2 and i±3 residues, depending on protein backbone rigidity and secondary structure elements. The mixing time should be set between 100-200 ms for uniformly labeled samples. All other values can be taken over from the short mixing time 2D ^{13}C-^{13}C PDSD.

3. Set up, record and process a 2D ^{15}N-^{13}C N_iCA_i and N_iCO_i experiment using a CP ^{1}H-^{15}N and a specific CP ^{15}N-^{13}C transfer[42]. Optimize the ^{15}N-^{13}C polarization transfer in a 1D fashion directly on the sample of interest, based on maximal intensity in the CA or carbonyl region, respectively. Typical values for the specific CP contact time are between 2-6 ms.
4. Set up, record and process a series of 2D ^{15}N-(^{13}C-)^{13}C experiments for the assignment purpose.
   Note: The first ^{15}N-^{13}C polarization transfer parameter value can be taken over from the N_iCA_i / N_iCO_i experiments. Intra-residue correlations are established from $N_i(CA_i)CB_i$ and $N_i(CA_i)CO_i$, using respectively DREAM[43] and PDSD ^{13}C-^{13}C polarization transfers. The residue (i) to residue (i-1) sequential connectivity is obtained from $N_i(CO_{i-1})CA_{i-1}$ and $N_i(CO_{i-1})CX_{i-1}$ experiments, both using a PDSD ^{13}C-^{13}C polarization transfer.
5. Choose an NMR analysis program such as CcpNmr analysis[44] or SPARKY[45]
6. Load the 2D spectra into the software (exemplified with CcpNmr analysis) and load the primary protein sequence.
7. Start with the identification of the amino acid types visible in the short-mixing ^{13}C-^{13}C PDSD spectrum. Connect the carbon atoms of the spin systems to allow for the "residue-type" specific assignment; see **Figure 4A** for the assignment of a Threonine residue. Identify as many residues as possible; this will depend on the protein subunit size, the spectral resolution and dispersion.
8. Overlay the short-mixing with the intermediate-mixing ^{13}C-^{13}C PDSD spectrum.
   NOTE: The supplementary peaks visible in the intermediate-mixing PDSD arise mostly from sequential (residue i - residue i±1) contacts. An example for a two-residue sequential assignment is illustrated in **Figure 4B**.
   1. Mark the resonance peaks of a spin system and find correlations in the intermediate-mixing PDSD with resonance frequencies of other spin systems. In small proteins or peptides, it can be possible to achieve the entire sequential resonance assignment based on 2D ^{13}C-^{13}C PDSD experiments.
      NOTE: In β-strand secondary structure motifs residue i - residue i±2 ^{13}C-^{13}C contacts might show more intense signals than sequential contacts due to their proximity in space; in α-helical secondary structure motifs residue i - residue i±3 ^{13}C-^{13}C contacts can also lead to intense signals.

9. If intermediate-mixing PDSD experiments on selectively ^{13}C-labeled samples are available, overlay them onto the short-mixing spectrum (if available on the selectively ^{13}C-labeled sample) and assign the supplemental peaks, taking into account the selective ^{13}C labeling pattern (1,3-^{13}C and 2-^{13}C glycerol[32,33] or 1-^{13}C and 2^{13}C glucose[29,30,31].
   NOTE: For example, in a 2-^{13}C glycerol labeled sample several amino acid types are labeled on the Cα position without the adjacent carbons (Cβ and C') labeled, therefore favoring the Cα-Cα transfer between adjacent residues. In selectively labeled samples, long-range ^{13}C-^{13}C correlations might build up already in intermediate-mixing ^{13}C-^{13}C PDSD experiments. If a peak cannot be explained by a sequential correlation, it could arise from a long-range contact. For highly ordered homogeneous subunit structures in the macromolecular assembly, only one set of resonances is expected to be visible in the spectra. If doubled (or further multiplied) resonances are visible for ^{13}C atoms or protein backbone stretches, two (or more) conformations for the atom or the primary sequence stretch in the assembly, respectively, exist.
10. Use the 2D NCA spectrum containing intra-residue ^{15}N-^{13}Cα correlations to identify the ^{15}N resonance frequencies for each residue. If the resolution in the ^{13}C dimension is not sufficient, use the supplementary information about the Cβ resonance in the 2D NCACB to identify the intra-residue ^{15}N resonance frequency.
11. Use the 2D NCACB and NCACO spectra containing intra-residue ^{15}N-^{13}C-^{13}C correlations to (i) identify the intra-residue ^{15}N frequency and (ii) to resolve ambiguities in the ^{13}C-^{13}C PDSD with the help of the additional ^{15}N dimension. The inversion of the signal due to the DREAM transfer leads to the observation of typical Cα-Cβ correlations for which the Cα signal is positive and the Cβ signal negative. Further side-chain ^{13}C, if visible in the spectrum, are positive again.

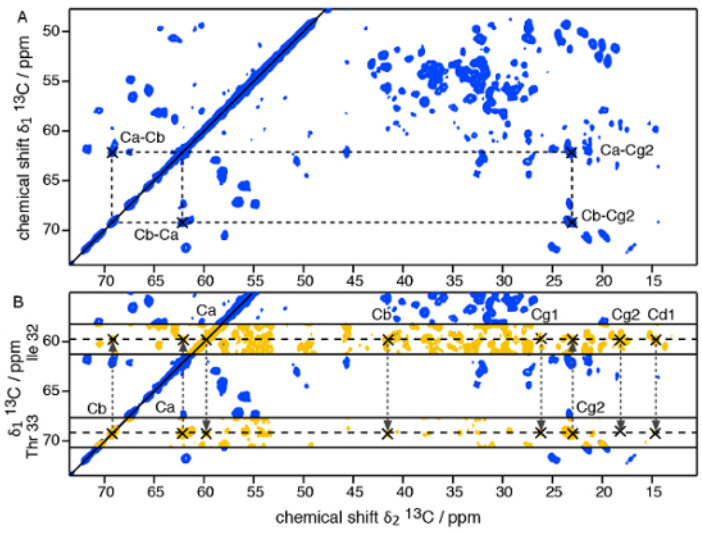

Figure 4: 2-dimensional ^{13}C- ^{13}C SSNMR PDSD experiments on a well-ordered, uniformly ^{13}C, ^{15}N-labeled protein assembly. A) Short mixing time PDSD (50 ms mixing). B) Assignment of the 2-residue stretch Ile32 - Thr33 using the overlay of the short mixing time PDSD with a long mixing time PDSD (200 ms mixing). Please click here to view a larger version of this figure.

2. **Secondary structure determination**
   1. Use ^{13}Cα, ^{13}Cβ chemical shift values to calculate the secondary chemical shift [46]ΔδCα-ΔδCβ, indicative of the secondary structure. Calculate ^{13}Cα(assigned)-^{13}Cα(random coil) and ^{13}Cβ(assigned)-^{13}Cβ(random coil).

NOTE: Chemical shift values for residues in random coil conformation can be obtained from[38].

1. Plot ΔδCα-ΔδCβ, negative or positive values for > 3 residues in a row indicate β-strand or α-helical conformation respectively; glycine and proline residues might show unusual chemical shift values, as they often act as "secondary structure breakers".

2. Predict the protein dihedral angles from the assigned chemical shifts using TALOS+[47,48] or PREDITOR[49,50]. The predicted Phi/Psi dihedral angles reflect the secondary structure of the protein subunit and are used as structural restraints throughout the modeling process.

3. **Collection of structural restraints**
   1. Set up and record a 2D ^{13}C-^{13}C PDSD experiment with a long mixing time to detect long-range ^{13}C-^{13}C correlations. Typical mixing times range from 400 ms to 1 s. Use selectively ^{13}C-labeled samples, as the spin dilution greatly improves the polarization transfer among distant carbons.
   2. Overlay the long-mixing 2D ^{13}C-^{13}C PDSD recorded on selectively labeled sample onto the intermediate-mixing ^{13}C-^{13}C PDSD, if possible recorded on the same selectively labeled sample. Supplemental peaks arise from correlations between more distant ^{13}C atoms. During resonance assignment, take into account the selective labeling scheme.
   3. Carefully evaluate the resolution of the spectrum to define an assignment tolerance window, *i.e.* dependent on the spectral resolution resonances in a certain ppm range this can contribute to the signal. The standard deviation of the assignment precision is automatically calculated in NMR assignment programs such as CcpNmr analysis or SPARKY.
   4. If a signal can be explained by a sequential (residue i - residue i±1) or a medium-range ^{13}C-^{13}C contact (residue i - residue i ± 2, 3 or 4), maintain this assignment since relayed polarization transfer can explain the correlation even if the ^{13}C-^{13}C distance is above the expected visible contact range.
   5. Classify the assignments of long-range ^{13}C-^{13}C contacts into frequency unambiguous and ambiguous signals. In the case of frequency unambiguous assignments, only one resonance assignment is possible with respect to the assignment tolerance window.
      NOTE: Ambiguous assignments contain all possible resonance assignments within the tolerance window. The ambiguities can be lifted simultaneously during the structure calculation by iterative rounds of disambiguation based on preliminary structures calculated using only the unambiguous restraints, as performed in computational routines such as ARIA[51] or UNIO[52]. Furthermore, structural data from different biophysical sources (*e.g.* mutated or truncated subunit structure by solution NMR or X-ray crystallography, mass-per-length measurements, cryo-EM map) can also be used to reduce the level of ambiguity, for examples see [1,3,53,54,55,56,57,58].

4. **Detection of intermolecular distance restraints in a symmetrical protein assembly**
   1. Set up a 2D ^{15}N-^{13}C PAIN-CP[59] experiment on a mixed (50/50) U-^{15}N- / U-^{13}C-labeled sample. Signals detected on the PAIN-CP spectrum should arise from inter-molecular ^{15}N-^{13}C proximities. Use the previously assigned resonances to perform the assignment of the intermolecular contacts.
   2. Set up a 2D ^{13}C-^{13}C PDSD with a long mixing time (>600 ms) on a (50/50) mixed (1,3-^{13}C)- / (2-^{13}C)-glycerol or (1-^{13}C)- / (2-^{13}C)-glucose sample.
      NOTE: Signals detected in this ^{13}C-^{13}C spectrum arise from intra-molecular and inter-molecular ^{13}C-^{13}C proximities. However, the high complementarity of the two labeling schemes lets particular resonance pairs arise unambiguously from inter-molecular contacts, e.g. a Serine CA in the (2-^{13}C)-glucose labeled subunits that correlate a Serine CB in the (1-^{13}C)-glucose labeled subunits.
      1. Overlay the spectrum of the mixed sample to the 2D ^{13}C-^{13}C spectra recorded on homogeneously labeled samples ((1,3-^{13}C)- and (2-^{13}C)-glycerol or (1-^{13}C)- and (2-^{13}C)-glucose labeled samples). Additional signals in the spectrum recorded on the mixed sample should arise from inter-molecular interactions.

5. **Structure modeling from SSNMR data**
   1. Prepare the SSNMR restraint lists needed for the structure calculation: (1) protein sequence; (2) intra-molecular unambiguous distance restraints; (3) intra-molecular ambiguous distance restraints; (4) TALOS-based dihedral angle restraints; (5) inter-molecular unambiguous distance restraints; (6) inter-molecular ambiguous distance restraints; (7) additional data from other biophysical techniques (*e.g.* mass-per-length, symmetry parameters).
   2. Several reviews provide insights into structure modeling based on SSNMR data and in conjunction with complementary structural data [14,60,15,19,61,62] Note that the ambiguous distance restraints can be disambiguated during structure calculation with respect to the preliminary structural models based on unambiguous distance restraints. To ensure structure accuracy, carefully observe if the structure converges to a single fold.

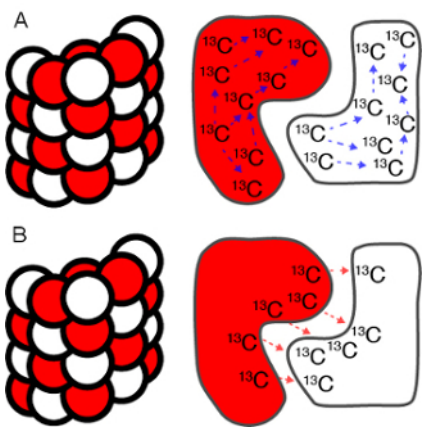

Figure 5: Intra- and intermolecular contacts in symmetric protein assemblies. Schematic representation of intra- *vs.* intermolecular ^{13}C-^{13}C long-range contacts in a helical macromolecular assembly. The subunits are colored in white and red to illustrate the mixed labeling of the subunits; *i.e.* before assembly a 1:1 mixture of two different labeling schemes was performed (*e.g.* 1-^{13}C glucose and 1-^{13}C glucose). **A**) Intramolecular ^{13}C-^{13}C long-range contacts (blue dashed arrow); **B**) intermolecular ^{13}C-^{13}C long-range contacts (red dashed arrows). Please click here to view a larger version of this figure.

Representative Results

The typical SSNMR workflow includes several steps illustrated in **Figure 1**. Usually the protein subunits are produced by *in vitro* heterologous expression in *E. coli*, purified and assembled under shaking but sometimes also in static conditions. Expression and purification of the protein subunit are followed by SDS gel chromatography (**Figure 2A**). The formation of macromolecular assemblies can then be confirmed by electron microscopy (EM) analysis (see **Figure 2B** for an example of a filamentous assembly).

After introduction of the protein assembly into the SSNMR rotor, the rotor is inserted into the spectrometer, the MAS frequency and temperature are regulated and the spectra are recorded. First insights can be obtained by 1D SSNMR techniques. **Figure 3** shows a typical SSNMR FID detected on the ^{13}C channel on a structurally homogeneous protein sample, a ^{1}H-^{13}C CP spectrum, revealing the ^{13}C resonances present in the rigid core of the protein subunit in the assembly, and a 2D ^{1}H-^{13}C INEPT spectrum, representing the mobile residues. For atomic insights into the rigid core of the assembly structure, multidimensional SSNMR experiments need to be recorded on uniformly and selectively labeled samples to first assign the SSNMR resonances and then detect long-range proximities (see **Figure 4**).

All spectra are processed and analyzed with adequate software to assign the SSNMR resonances and extract intra- and intermolecular distance restraints (**Figure 5**). The SSNMR distance restraints are either used alone or in conjunction with data from complementary techniques, which can be integrated into the modeling program.

For representative atomic structures of macromolecular assemblies solved by SSNMR techniques **Figure 6** illustrates several filamentous assemblies from bacterial appendages and amyloid fibrils.

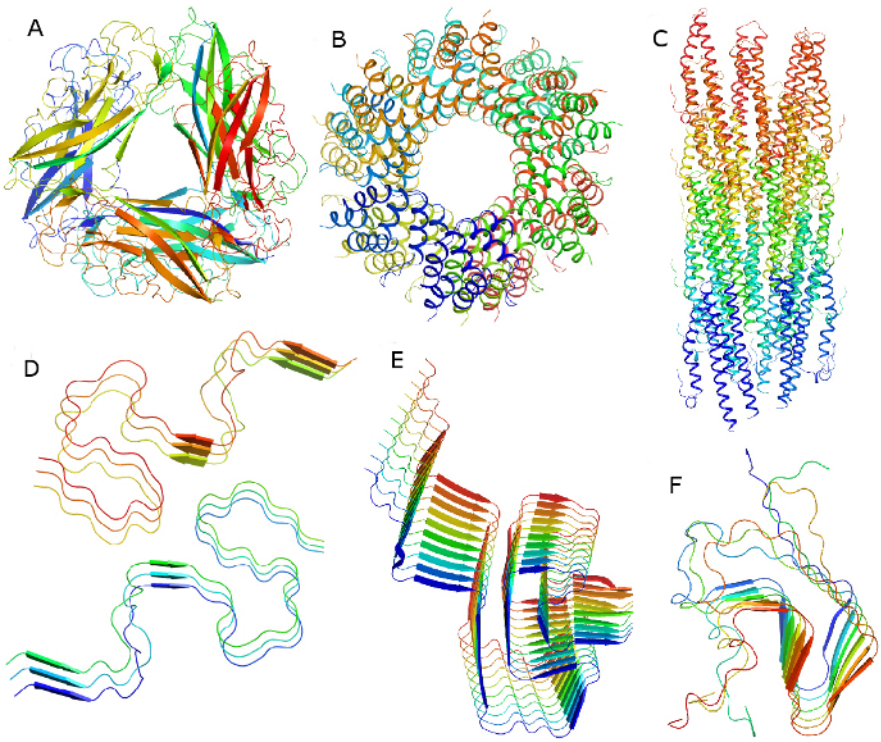

Figure 6:**Filamentous macromolecular structures determined by a solid-state NMR approach: bacterial filaments and amyloid protein fibrils.A)** Type 1 pilus of uropathogenic *E. coli*, PDB code 2N7H [4]; **B**) ASC filament, PDB code 2N1F [63]; **C**) Type III secretion system needles, PDB codes 2MME, 2LPZ and 2MEX [2,3,64]; **D**) Amyloid-beta AB42 fibrils, PDB code 2NAO, 5KK3, 2MXU [65,66,67] and Osaka mutant PDB code 2MVX [57], Iowa mutant PDB code 2MPZ [58]; **E**) Alpha-synuclein fibrils, PDB code 2N0A [68]; **F**) HET-s prion domain, PDB code 2RNM, 2KJ3 [69,70]. Please click here to view a larger version of this figure.

Discussion

Solid-state NMR (SSNMR) is a method of choice for characterizing macromolecular protein assemblies at an atomic level. One of the central issues in SSNMR-based structure determination is the spectral quality of the investigated system, that allows establishing 3D structural models of various precision, typically ranging from low-resolution models (containing the secondary structure elements and little 3D information) to

pseudo-atomic 3D structures. The quantity and quality of structural information extracted from multi-dimensional SSNMR experiments is the key to compute a high-resolution NMR structure of the assembly.

The described protocol relies on the detection of ^{13}C-^{13}C and ^{15}N-^{13}C structural restraints requiring the recording of several 2D (and sometimes 3D) spectra with high signal-to-noise. At moderate MAS frequencies (<25 kHz), the sample is introduced into rotors with sizes of 3.2-4 mm diameter allowing for protein quantities of up to ~50 mg, dependent on the sample hydration. The amount of sample inside the rotor is directly proportional to the signal-to-noise ratio in SSNMR spectra, a decisive factor for the detection of long-range distance restraints and their unambiguous assignment.

The spectral resolution is a crucial parameter during the sequential resonance assignment and the restraints collection. To obtain optimal results, the sample preparation parameters need to be optimized, particularly in the purification of the subunit and the assembly conditions (pH, buffer, shaking, temperature, *etc.*). For sample optimization, it is recommended to prepare unlabeled samples for several distinct conditions for which assembly has been observed, and to record a 1D ^{1}H-^{13}C CP spectrum (described in step 2.1) on each prepared sample. The spectra serve to compare spectral resolution and dispersion between the different preparations, based upon which the optimal conditions can be determined.

The quality of the SSNMR data depends strongly on the choice of the NMR acquisition parameters, especially for the polarization transfer steps. The use of high magnetic field strengths (≥600 MHz ^{1}H frequency) is essential for high sensitivity and spectral resolution, required when facing complex targets such as macromolecular protein assemblies.

A limiting factor in many cases is the spectrometer availability. Therefore, a judicious choice of the samples to be prepared should precede the spectrometer session. In any case, a uniformly ^{13}C, ^{15}N-labeled sample is a prerequisite to perform the sequential and intra-residual resonance assignment. For proteins assigned by solid-state NMR techniques see[71]. Structure determination of macromolecular assemblies at moderate MAS frequencies requires selectively ^{13}C-labeled samples; for the detection of long-range ^{13}C-^{13}C and ^{13}C-^{15}N contacts samples based on 1,3-^{13}C- and 2-^{13}C-gylcerol and/or 1-^{13}C - and 2-^{13}C-glucose labeling are commonly used, as described above. The choice between the two labeling schemes is based on the spectral signal-to-noise ratio and resolution. To distinguish between intra- and intermolecular long-range contacts, mixed labeled and diluted samples have revealed efficient.

In short, the critical steps for an atomic SSNMR structural study are: (i) the preparation of the subunits and the assembly need to be optimized to obtain excellent sample quantity and quality, (ii) spectrometer field strength and acquisition parameters have to be chosen carefully; (iii) selective labeling strategies are required for a 3D structure determination and the amount of required data depends on data quality and the availability of complementary data.

Despite its applicability to a wide range of supramolecular systems ranging from membrane proteins to homomultimeric nano-objects, SSNMR is often limited by the need for mg-quantities of isotopically labeled material. The recent technological developments in ultra-fast MAS (≥100 kHz) SSNMR open up the avenue to ^{1}H-detected NMR, and push the limit of minimal sample quantity to sub-mg [72,73,74]. Nevertheless, for detailed structural studies ^{13}C-labeled samples are indispensable, which limits the application of SSNMR to samples assembled *in vitro* or to systems expressed in organisms that survive on minimal medium where in-cell SSNMR is an emerging method (for reviews see [75,76,77,78]).

An important factor in SSNMR application to obtain high-resolution 3D structures is the spectral resolution: intrinsic conformational heterogeneity in an assembly can limit spectral resolution and spectra analysis. Residue specific ^{13}C labeling may in some cases provide an alternative to obtain specific distance information on strategic residues in order to obtain structural models (for a recent examples see [79,80]).

SSNMR for 3D structure determination still requires the collection of several datasets with often long data collection times on sophisticated instruments, depending on the approach and the system several days to weeks on a 600-1000 MHz (^{1}H frequency) spectrometer. Therefore, the access to spectrometer time can be a limiting factor in an in-depth SSNMR study.

In the case of homomultimeric protein assemblies, leading to SSNMR data of sufficient quality to identify a high number of structural restraints such as in [3,57,64,70], SSNMR still gives no access to the microscopic dimensions. Therefore, in a *de novo* SSNMR structure determination of a homomultimeric assembly, EM or mass-per-length (MPL) data ideally complement SSNMR data to derive the symmetry parameters. SSNMR data alone provide the atomic intra- and intermolecular interfaces

SSNMR is highly complementary with structural techniques such as EM or MPL measurements but the data can also perfectly be combined with atomic structures obtained by X-ray crystallography or solution NMR on mutated or truncated subunits. An increasing number of studies can be found in literature where the conjunction of different structural data has allowed for determining atomic 3D models of macromolecular assemblies (see **Figure 6** for representative examples).

In the field of Structural Biology, SSNMR emerges as promising technique to study insoluble and non-crystalline assemblies at the atomic level, *i.e.* providing structural data at the atomic scale. In this respect, SSNMR is the pendant to solution NMR and X-ray crystallography for molecular assemblies, including membrane proteins in their native environment and protein assemblies such as viral envelopes, bacterial filaments or amyloids, as well as RNA and RNA-protein complexes (see for example[81]). Its highly versatile applications *in vitro* and in the cellular context, such as tracking secondary, tertiary and quaternary structural changes, identifying interaction surfaces with partner molecules on the atomic scale (for example [82]) and mapping molecular dynamics in the context of assembled complexes, indicate the important potential of SSNMR in future structural studies on complex biomolecular assemblies.

Component	M9 medium
NaCl	0.5 g/L
KH_2PO_4	3 g/L
Na_2HPO_4	6.7 g/L
$MgSO_4$	1 mM
$ZnCl_2$	10 µM
$FeCl_3$	1 µM
$CaCl_2$	100 µM
MEM vitamin mix 100X	10 mL/L
^{13}C-glucose	2 g/L
$^{15}NH_4Cl$	1 g/L

Table 1: Composition of minimal expression medium for recombinant protein production in *E. coli* BL21 cells.

Disclosures

The authors have nothing to disclose.

Acknowledgements

This work is funded by the ANR (13-PDOC-0017-01 to B.H. and ANR-14-CE09-0020-01 to A.L.), "Investments for the future" Programme IdEx Bordeaux/CNRS (PEPS 2016 to B.H.) reference ANR-10-IDEX-03-02 to B.H., the Fondation pour la Recherche Médicale (FRM-AJE20140630090 to A.L.), the FP7 program (FP7-PEOPLE-2013-CIG to A.L.) and the European Research Council (ERC) under the European Union's Horizon 2020 research and innovation program (ERC Starting Grant to A.L., agreement No 639020) and project "WEAKINTERACT."

References

1. Morag, O., Sgourakis, N. G., Baker, D., Goldbourt, A. The NMR-Rosetta capsid model of M13 bacteriophage reveals a quadrupled hydrophobic packing epitope. *Proc Natl Acad Sci U S A.* **112** (4), 971-976 (2015).
2. Loquet, A. *et al.* Atomic model of the type III secretion system needle. *Nature.* **486** (7402), 276-279 (2012).
3. Demers, J. P. *et al.* High-resolution structure of the Shigella type-III secretion needle by solid-state NMR and cryo-electron microscopy. *Nat Commun.* **5** (4976) (2014).
4. Habenstein, B. *et al.* Hybrid Structure of the Type 1 Pilus of Uropathogenic Escherichia coli. *Angew Chem Int Ed Engl.* **54** (40), 11691-11695 (2015).
5. Cady, S. D. *et al.* Structure of the amantadine binding site of influenza M2 proton channels in lipid bilayers. *Nature.* **463** (7281), 689-692 (2010).
6. Möllers, K. B., Park, S. H. *et al.* Structure of the chemokine receptor CXCR1 in phospholipid bilayers. *Nature.* **491** (7426), 779-783 (2012).
7. Kaplan, M. *et al.* Probing a cell-embedded megadalton protein complex by DNP-supported solid-state NMR. *Nat Methods.* **12** (7), 649-652 (2015).
8. Wang, S. *et al.* Solid-state NMR spectroscopy structure determination of a lipid-embedded heptahelical membrane protein. *Nat Methods.* **10** (10), 1007-1012 (2013).
9. Daskalov, A. *et al.* Signal transduction by a fungal NOD-like receptor based on propagation of a prion amyloid fold. *PLoS Biol.* **13** (2), e1002059 (2015).
10. Daskalov, A. *et al.* Identification of a novel cell death-inducing domain reveals that fungal amyloid-controlled cell death is related to necroptosis. *Proc Natl Acad Sci U S A.* (2016).
11. Li, J. *et al.* The RIP1/RIP3 necrosome forms a functional amyloid signaling complex required for programmed necrosis. *Cell.* **150** (2), 339-350 (2012).
12. Knowles, T. P., Vendruscolo, M., Dobson, C. M. The amyloid state and its association with protein misfolding diseases. *Nat Rev Mol Cell Biol.* **15** (6), 384-396 (2014).
13. Aguzzi, A., Lakkaraju, A. K. Cell Biology of Prions and Prionoids: A Status Report. *Trends Cell Biol.* **26** (1), 40-51 (2016).
14. Habenstein, B., Loquet, A. Solid-state NMR: An emerging technique in structural biology of self-assemblies. *Biophys Chem.* (2015).
15. Meier, B. H., Bockmann, A. The structure of fibrils from 'misfolded' proteins. *Curr Opin Struct Biol.* **30** 43-49 (2015).
16. Miao, Y., Cross, T. A. Solid state NMR and protein-protein interactions in membranes. *Curr Opin Struct Biol.* **23** (6), 919-928 (2013).
17. Tang, M., Comellas, G., Rienstra, C. M. Advanced solid-state NMR approaches for structure determination of membrane proteins and amyloid fibrils. *Acc Chem Res.* **46** (9), 2080-2088 (2013).
18. Weingarth, M., Baldus, M. Solid-state NMR-based approaches for supramolecular structure elucidation. *Acc Chem Res.* **46** (9), 2037-2046 (2013).
19. Loquet, A., Habenstein, B., Lange, A. Structural investigations of molecular machines by solid-state NMR. *Acc Chem Res.* **46** (9), 2070-2079 (2013).

20. Yan, S., Suiter, C. L., Hou, G., Zhang, H., Polenova, T. Probing structure and dynamics of protein assemblies by magic angle spinning NMR spectroscopy. *Acc Chem Res.* **46** (9), 2047-2058 (2013).
21. Tycko, R., Wickner, R. B. Molecular structures of amyloid and prion fibrils: consensus versus controversy. *Acc Chem Res.* **46** (7), 1487-1496 (2013).
22. Hong, M., Zhang, Y., Hu, F. Membrane protein structure and dynamics from NMR spectroscopy. *Annu Rev Phys Chem.* **63** 1-24 (2012).
23. Jelinek, R., Ramamoorthy, A., Opella, S. J. High-Resolution Three-Dimensional Solid-state NMR Spectroscopy of a Uniformly 15N-Labeled Protein *J Am Chem Soc.* **117** 12348-12349 (1995).
24. Xu, J. *et al.* Bicelle-enabled structural studies on a membrane-associated cytochrome B5 by solid-state MAS NMR spectroscopy. *Angew Chem Int Ed Engl.* **47** (41), 7864-7867 (2008).
25. Durr, U. H., Gildenberg, M., Ramamoorthy, A. The magic of bicelles lights up membrane protein structure. *Chem Rev.* **112** (11), 6054-6074 (2012).
26. Yamamoto, K. *et al.* Probing the transmembrane structure and topology of microsomal cytochrome-p450 by solid-state NMR on temperature-resistant bicelles. *Sci Rep.* **3** 2556 (2013).
27. Huang, R. *et al.* Probing the transmembrane structure and dynamics of microsomal NADPH-cytochrome P450 oxidoreductase by solid-state NMR. *Biophys J.* **106** (10), 2126-2133 (2014).
28. Durr, U. H., Yamamoto, K., Im, S. C., Waskell, L., Ramamoorthy, A. Solid-state NMR reveals structural and dynamical properties of a membrane-anchored electron-carrier protein, cytochrome b5. *J Am Chem Soc.* **129** (21), 6670-6671 (2007).
29. Hong, M. Determination of multiple phi-torsion angles in proteins by selective and extensive (13)C labeling and two-dimensional solid-state NMR. *J Magn Reson.* **139** (2), 389-401 (1999).
30. Lundstrom, P. *et al.* Fractional 13C enrichment of isolated carbons using [1-13C]- or [2- 13C]-glucose facilitates the accurate measurement of dynamics at backbone Calpha and side-chain methyl positions in proteins. *J Biomol NMR.* **38** (3), 199-212 (2007).
31. Loquet, A., Lv, G., Giller, K., Becker, S., Lange, A. 13C spin dilution for simplified and complete solid-state NMR resonance assignment of insoluble biological assemblies. *J Am Chem Soc.* **133** (13), 4722-4725 (2011).
32. Castellani, F. *et al.* Structure of a protein determined by solid-state magic-angle-spinning NMR spectroscopy. *Nature.* **420** (6911), 98-102 (2002).
33. Higman, V. A. *et al.* Assigning large proteins in the solid state: a MAS NMR resonance assignment strategy using selectively and extensively 13C-labelled proteins. *J Biomol NMR.* **44** (4), 245-260 (2009).
34. Bockmann, A. *et al.* Characterization of different water pools in solid-state NMR protein samples. *J Biomol NMR.* **45** (3), 319-327 (2009).
35. Cavanagh, J., Fairbrother, W. J., Palmer, A. G., Skelton, N. J. *Protein NMR spectroscopy, principles and practice*., Academic, San Diego, (1996).
36. Hartman, S. R., Hahn, E. L. Nuclear Double Resonance in the Rotating Frame. *Phys Rev.* **128** (5), 2042-2053 (1962).
37. Harris, R. K. *et al.* Further conventions for NMR shielding and chemical shifts IUPAC recommendations 2008. *Solid State Nucl Magn Reson.* **33** (3), 41-56 (2008).
38. Wang, Y., Jardetzky, O. Probability-based protein secondary structure identification using combined NMR chemical-shift data. *Protein Sci.* **11** (4), 852-861 (2002).
39. Shaka, A. J., Baker, P. B., Freeman, R. Computer-Optimized Scheme for Wideband Applications and Low-Level Operation. *J Magn Reson.* **64** 547-552 (1985).
40. *Biological Magnetic Resonance Bank.* http://bmrb.wisc.edu/. Accessed May 15 (2017).
41. Szeverenyi, N. M., Sullivan, M. J., Maciel, G. E. Observation of Spin Exchange by Two-Dimensional Fourier-Transform C-13 Cross Polarization-Magic-Angle Spinning. *J Magn Reson.* **47** 462-475 (1982).
42. Baldus, M., Petkova, A. T., Herzfeld, J., Griffin, R. G. Cross polarization in the tilted frame: assignment and spectral simplification in heteronuclear spin systems. *Mol Phys.* **95** (5), 1197-1207 (1998).
43. Verel, R., Ernst, M., Meier, B. H. Adiabatic dipolar recoupling in solid-state NMR: the DREAM scheme. *J Magn Reson.* **150** (1), 81-99 (2001).
44. *CcpNmr Analysis - Collaborative Computational Project for NMR.* http://www.ccpn.ac.uk/software/analysis. Accessed May 15 (2017).
45. *Sparky - NMR Assignment and Integration Software.* https://www.cgl.ucsf.edu/home/sparky/. Accessed May 15 (2017).
46. Luca, S. *et al.* Secondary chemical shifts in immobilized peptides and proteins: a qualitative basis for structure refinement under magic angle spinning. *J Biomol NMR.* **20** (4), 325-331 (2001).
47. *TALOS+: Prediction of Protein Backbone Torsion Angles from NMR Chemical Shifts.* http://spin.niddk.nih.gov/bax/software/TALOS/. Accessed May 15 (2017).
48. Shen, Y., Bax, A. SPARTA+: a modest improvement in empirical NMR chemical shift prediction by means of an artificial neural network. *J Biomol NMR.* **48** (1), 13-22 (2010).
49. *Dihedral angles from chemical shifts and homology.* http://wishart.biology.ualberta.ca/shiftor/. Accessed May 15 (2017).
50. Berjanskii, M. V., Neal, S., Wishart, D. S. PREDITOR: a web server for predicting protein torsion angle restraints. *Nucleic Acids Res.* **34** (Web Server issue), W63-69 (2006).
51. Bardiaux, B., Malliavin, T., Nilges, M. ARIA for solution and solid-state NMR. *Methods Mol Biol.* **831** 453-483 (2012).
52. Guerry, P., Herrmann, T. Comprehensive automation for NMR structure determination of proteins. *Methods Mol Biol.* **831** 429-451 (2012).
53. Vasa, S. *et al.* beta-Helical architecture of cytoskeletal bactofilin filaments revealed by solid-state NMR. *Proc Natl Acad Sci U S A.* **112** (2), E127-136 (2015).
54. He, L. *et al.* Structure determination of helical filaments by solid-state NMR spectroscopy. *Proc Natl Acad Sci U S A.* **113** (3), E272-281 (2016).
55. Tang, M. *et al.* High-resolution membrane protein structure by joint calculations with solid-state NMR and X-ray experimental data. *J Biomol NMR.* **51** (3), 227-233 (2011).
56. Paravastu, A. K., Leapman, R. D., Yau, W. M., Tycko, R. Molecular structural basis for polymorphism in Alzheimer's beta-amyloid fibrils. *Proc Natl Acad Sci U S A.* **105** (47), 18349-18354 (2008).
57. Schutz, A. K. *et al.* Atomic-resolution three-dimensional structure of amyloid beta fibrils bearing the Osaka mutation. *Angew Chem Int Ed Engl.* **54** (1), 331-335 (2015).
58. Sgourakis, N. G., Yau, W. M., Qiang, W. Modeling an in-register, parallel "iowa" abeta fibril structure using solid-state NMR data from labeled samples with rosetta. *Structure.* **23** (1), 216-227 (2015).
59. Lewandowski, J. R., De Paepe, G., Griffin, R. G. Proton assisted insensitive nuclei cross polarization. *J Am Chem Soc.* **129** (4), 728-729 (2007).

60. Carlon, A. *et al.* How to tackle protein structural data from solution and solid state: An integrated approach. *Prog Nucl Magn Reson Spectrosc.* **92-93** 54-70 (2016).
61. Judge, P. J., Taylor, G. F., Dannatt, H. R., Watts, A. Solid-state nuclear magnetic resonance spectroscopy for membrane protein structure determination. *Methods Mol Biol.* **1261** 331-347 (2015).
62. Wang, S., Ladizhansky, V. Recent advances in magic angle spinning solid state NMR of membrane proteins. *Prog Nucl Magn Reson Spectrosc.* **82** 1-26 (2014).
63. Sborgi, L. *et al.* Structure and assembly of the mouse ASC inflammasome by combined NMR spectroscopy and cryo-electron microscopy. *Proc Natl Acad Sci U S A.* **112** (43), 13237-13242 (2015).
64. Loquet, A. *et al.* Atomic structure and handedness of the building block of a biological assembly. *J Am Chem Soc.* **135** (51), 19135-19138 (2013).
65. Walti, M. A. *et al.* Atomic-resolution structure of a disease-relevant Abeta(1-42) amyloid fibril. *Proc Natl Acad Sci U S A.* **113** (34), E4976-4984 (2016).
66. Colvin, M. T. *et al.* Atomic Resolution Structure of Monomorphic Abeta42 Amyloid Fibrils. *J Am Chem Soc.* **138** (30), 9663-9674 (2016).
67. Xiao, Y. *et al.* Abeta(1-42) fibril structure illuminates self-recognition and replication of amyloid in Alzheimer's disease. *Nat Struct Mol Biol.* **22** (6), 499-505 (2015).
68. Tuttle, M. D. *et al.* Solid-state NMR structure of a pathogenic fibril of full-length human alpha-synuclein. *Nat Struct Mol Biol.* **23** (5), 409-415 (2016).
69. Wasmer, C. *et al.* Amyloid fibrils of the HET-s(218-289) prion form a beta solenoid with a triangular hydrophobic core. *Science.* **319** (5869), 1523-1526 (2008).
70. Van Melckebeke, H. *et al.* Atomic-resolution three-dimensional structure of HET-s(218-289) amyloid fibrils by solid-state NMR spectroscopy. *J Am Chem Soc.* **132** (39), 13765-13775 (2010).
71. *BMRB Solid-state NMR entries.* http://www.bmrb.wisc.edu/data_library/solidstate.shtml. Accessed May 15 (2017).
72. Lamley, J. M. *et al.* Solid-state NMR of a protein in a precipitated complex with a full-length antibody. *J Am Chem Soc.* **136** (48), 16800-16806 (2014).
73. Agarwal, V. *et al.* De novo 3D structure determination from sub-milligram protein samples by solid-state 100 kHz MAS NMR spectroscopy. *Angew Chem Int Ed Engl.* **53** (45), 12253-12256 (2014).
74. Stanek, J. *et al.* NMR Spectroscopic Assignment of Backbone and Side-Chain Protons in Fully Protonated Proteins: Microcrystals, Sedimented Assemblies, and Amyloid Fibrils. *Angew Chem Int Ed Engl.* **55** (50), 15504-15509 (2016).
75. Baker, L. A., Baldus, M. Characterization of membrane protein function by solid-state NMR spectroscopy. *Curr Opin Struct Biol.* **27** 48-55 (2014).
76. Luchinat, E., Banci, L. In-cell NMR: a topical review. *IUCrJ.* **4** (Pt 2), 108-118 (2017).
77. Freedberg, D. I., Selenko, P. Live cell NMR. *Annu Rev Biophys.* **43** 171-192 (2014).
78. Selenko, P., Wagner, G. Looking into live cells with in-cell NMR spectroscopy. *J Struct Biol.* **158** (2), 244-253 (2007).
79. Qiang, W., Yau, W. M., Luo, Y., Mattson, M. P., Tycko, R. Antiparallel beta-sheet architecture in Iowa-mutant beta-amyloid fibrils. *Proc Natl Acad Sci U S A.* **109** (12), 4443-4448 (2012).
80. Bateman, D. A., Tycko, R., Wickner, R. B. Experimentally derived structural constraints for amyloid fibrils of wild-type transthyretin. *Biophys J.* **101** (10), 2485-2492 (2011).
81. Marchanka, A., Simon, B., Althoff-Ospelt, G., Carlomagno, T. RNA structure determination by solid-state NMR spectroscopy. *Nat Commun.* **6** 7024 (2015).
82. Schutz, A. K. *et al.* The amyloid-Congo red interface at atomic resolution. *Angew Chem Int Ed Engl.* **50** (26), 5956-5960 (2011).